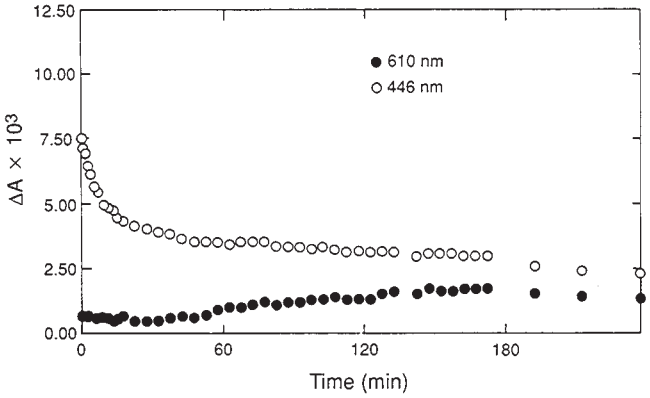

FIG. 3 Time-dependent absorbance changes at wavelengths characteristic of Py^+ (446 nm, ○), and MV^+ (610 nm, ●), following irradiation of the Py (4×10^{-5} M), TV^{+2} (0.5 mM in 40-mM NaCl), MV^{+2} (3×10^{-6} M) system. Other conditions were as in Fig. 2. The initial decay at 446 nm and increase at 610 nm are due to the superimposed contributions of reactions (4) and (5). The tailing slow decay above ~200 min is due to reaction (6).

minutes. This reaction, which most probably involves solvated electrons generated by photoionization of Py* (ref. 18), is still under investigation. Nevertheless, because side reactions, for example with water, shorten the lifetime of the electron, that process decays and allows the stabler TV^+ to reduce MV^{2+} molecules at much longer distances. We also note that a broad low-intensity peak at 380 nm (attributed to a photodecomposition product of TV^{2+}) grows over a timescale of several hours without, however, affecting the Py^+ and MV^+ absorptions.

We have thus achieved an extremely long lifetime of the photoinduced charge-separated pair, although in low yield, by immobilizing the primary donor and secondary acceptor in the rigid glass matrix. When treated as a bimolecular process, an upper limit of the rate of charge recombination through reaction (6) yields a second-order rate constant of $k(6)\leq 5\times10^2$ mol l^{-1} s^{-1} (obtained at $[MV^{2+}]=3\times10^{-6}$ M and at an ionic strength of 40 mM NaCl, the lifetime being independent of the ionic strength). This rate constant is seven orders of magnitude lower than in homogeneous methanolic solutions ($\sim5\times10^9$ mol^{-1} l^{-1} s^{-1})[15,19]. The retardation of the back-reaction in the present (ternary) trapped system is also at least two orders of magnitude more efficient than that seen[15] in the absence of a shuttler, using trapped Py and adsorbed MV^{2+}. In most previous attempts to achieve long-lived charge separation, there has been some degree of diffusional freedom allowing the back-reaction. This applies to flexible organic polymeric systems, to colloids and to systems based on adsorption[2,3]. The ability to block the diffusion process in the inert inorganic sol-gel matrix, while still allowing the diffusion of a mediating molecule, is the key to the success of the present system. □

Received 26 July; accepted 12 November 1991.

1. *Antennas and Reaction Centers of Photosynthetic Bacteria* (ed. Michel-Beyerle, M. E.) (Springer, Berlin, 1985).
2. *Photoinduced Electron Transfer* (eds Fox, M. A. & Chanon, M.) (Elsevier, Amsterdam, 1988).
3. Gratzel, M. *Heterogeneous Photochemical Electron Transfer* (CRC, Boca Raton, 1989).
4. *Photochemical Energy Conversion* (eds Norris, J. R. & Meisel, D.).
5. Brinker, C. J. & Scherer, G. *Sol-gel Science* (Academic, San Diego, 1990).
6. Slama-Schwok, A., Avnir, D. & Ottolenghi, M. (1991). *J. Am. chem. Soc.* **113,** 3984–3985 (1991).
7. Matsuo, T. *J. Photochem.* **29,** 41–54 (1985).
8. Adar, E., Degani, Y., Goren, Z. & Willner, I. *J. Am. chem. Soc.* **108,** 4696–4700 (1986).
9. Rabani, J. & Sassoon, R. E. *J. Photochem.* **29,** 726 (1985).
10. Margerum, L. D., Murray, R. W. & Meyer, T. J. *J. phys. Chem.* **90,** 728–730 (1986).
11. Moser, J., Gratzel, M. & Gallay, R. *Helv. chim. Acta* **70,** 1596–1604 (1987).
12. Anderson, R. F. *Ber. Bunseng. Phys. Chem.* **80,** 969–972 (1976).
13. Avnir, D., Ottolenghi, M. & Braun, S. in *Supramolecular Architecture in Two and Three Dimensions, ACS Symp. Series* (ed. Bein, T.) (American Chemical Society, in the press).
14. Slama-Schwok, A., Avnir, D. & Ottolenghi, M. *J. phys. Chem.* **93,** 7544–7547 (1989).
15. Slama-Schwok, A., Avnir, D. & Ottolenghi, M. *Photochem. Photobiol.* **54,** 525 (1991).
16. Grellman, K. H., Watkins, A. R. & Weller, A. *J. Luminesc.* **1/2,** 678–692 (1970).
17. Tsakahara, K. & Wilkins, R. G. *J. Am. chem. Soc.* **107,** 2632–2635 (1985).
18. Ottolenghi, M. *Chem. Phys. Lett.* **12,** 339–342 (1971).
19. Das, P. K. *J. Chem. Soc. Faraday Trans.* **79,** 1135–1145 (1983).
20. Homer, R. F. & Tomlinson, T. E. *J. chem. Soc.* 2498 (1960).

ACKNOWLEDGEMENTS. We are grateful to I. Willner, D. Mandler, N. Lapidot and Y. Eichen for a donation of TV^{2+} and for helpful discussions. We thank M. Grätzel for comments. The research was supported by grants from the Israel National Council for Research and Development, the US Army Research, Development and Standardization Group (UK), the E. Berman Research Fund and the Krupp Foundation. Support by the L. Farkas (Minerva) Center for Light-Energy Conversion and by the F. Haber Research Center for Molecular Dynamics is also acknowledged.

A polymer gel with electrically driven motility

Yoshihito Osada, Hidenori Okuzaki & Hirofumi Hori

Department of Chemistry, Ibaraki University, 2-1-1 Bunkyo, Mito, Ibaraki 310, Japan

A SYSTEM capable of converting chemical energy to mechanical energy could serve as an actuator or an 'artificial muscle' in several applications. Here we describe a chemomechanical system of this sort based on a synthetic polymer gel. The gel network is anionic, and positively charged surfactant molecules can therefore bind to its surface, inducing local shrinkage by decreasing the difference in osmotic pressure between the gel interior and the solution outside. By using an electric field to direct surfactant binding selectively to one side of the gel, we can induce contraction and curvature of a strip of gel. Reversing the direction of the field causes contraction of the opposite side, and when the gel is suspended in solution from a ratchet mechanism, it can thereby be made to move with a worm-like motion at a velocity of up to 25 cm min^{-1}.

The isothermal conversion of chemical energy into mechanical work underlies the motility of all living organisms. These systems are efficient because chemical energy is directly converted to mechanical energy without intermediate steps producing heat. Early this century, J. H. van't Hoff showed that chemical free energy could in theory be converted into mechanical work by osmotic cells with pistons. Van't Hoff's theoretical osmotic engine is, of course, very different from living muscles, where the motility is produced by an appropriate assembly of protein molecules.

More than 40 years ago, Katchalsky and collaborators[1,2] demonstrated that collagen fibres changed dimension reversibly on transition from cyclic helices to random coils when they were immersed cyclically in salt solution and water. Katchalsky *et al.* referred to this as a 'mechanochemical system', defined as a thermodynamic system capable of transforming chemical energy to mechanical work (nowadays, the term 'chemomechanical system' is preferred). Since then, there have been few advances in practical chemomechanical devices, except for some constructional modifications[3].

We report here a model of an electrically driven 'muscle', made of water-swollen synthetic polymer gel, which has motility when immersed in water. The system is based on an electrokinetic molecular assembly reaction of surfactant molecules on the hydrogel, which is made of weakly crosslinked poly(2-acrylamido-2-methyl propane) sulphonic acid (PAMPS).

PAMPS gel was prepared by radical polymerization in the presence of 5 mol% crosslinking agent, *N,N'*-methylene bisacrylamide, as described previously[4,5]. A strip of PAMPS gel, 1 mm thick, 5 mm wide and 20 mm long, was made, and a pair of plastic hooks which act as pawls were attached to the ends. The strip was suspended from a long plastic ratchet bar, and then immersed in a dilute solution of the surfactant, *n*-dodecyl pyridinium chloride ($C_{12}PyCl$) containing 3×10^{-2} M sodium sulphate (Fig. 1). The gel swelled by a factor of 45 in this solution compared with its dry weight.

We applied a d.c. voltage of 20 V through a pair of planar carbon electrodes (450 mm long, 10 mm wide, 1 mm thick)

placed in the solution 4 mm above and 16 mm below the top of the ratchet bar, thus producing a field of 10 V cm^{-1} and a current of 15 mA cm^{-2}, and altered the polarity at 2-s intervals. This made the gel move forward with a 'looping' action by repeated bending and stretching. Figure 1 shows successive profiles of the 'gel-looper' as it walks with a constant velocity of 25 cm min^{-1} in the solution.

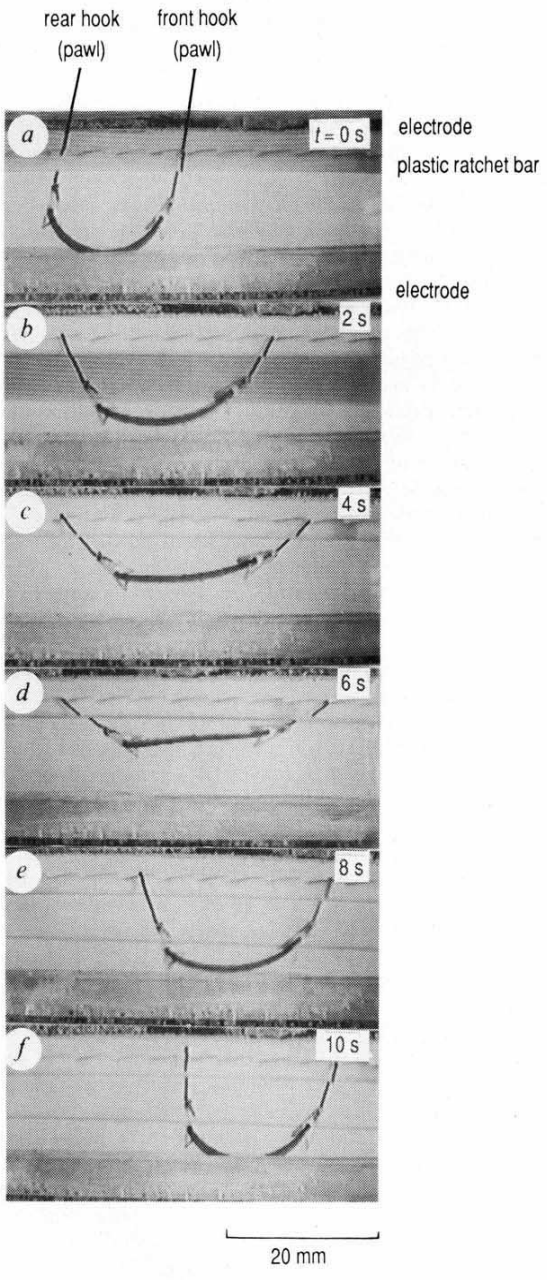

FIG. 1 Time profiles of the polymer gel in action. *a–d*, 'Stretching' process. The front hook attached to the gel can slide forward along the plastic ratchet bar, but the rear hook is prevented by the teeth of the ratchet from sliding backwards. *e*, *f*, Bending process. When the polarity of the electric field is reversed and the gel bends, the rear hook can move forward along the ratchet bar, but the front hook is prevented from sliding backwards. This action being repeated, the gel walks forward. The gel is poly(2-acrylamido-2-methyl propane) sulphonic acid (PAMPS); degree of crosslinking 5 mol%; degree of swelling in the solution, a factor of 45. Electric field, 20 V; current 15 mA cm^{-2}; electrode distance, 20 mm. Solution: 1×10^{-2} M *n*-dodecylpyridinium chloride, containing 3×10^{-2} M sodium sulphate. Total ionic strength: 0.1.

The walking velocity is a function of the applied current, the salt concentrations of surfactant and sodium sulphate, and the molecular size of alkyl chains of surfactant molecules. The velocity increased with increasing current, but there existed optimum sodium sulphate and surfactant concentrations: the maximum velocity of 25 cm min^{-1} occurred at concentrations of 3×10^{-2} M sodium sulphate and 1×10^{-2} M C_{12}PyCl at 20 V d.c. Any increase or decrease of concentrations decreased the motility.

The principle of the gel's motility lies in a reversible and cooperative complexing of surfactant molecules on the polymer gel in an electric field, causing the gel to shrink. As is well established[6], swelling of the ionic gel is characterized by the difference between the osmotic pressure of freely mobile ions in the gel and in the surrounding solution, and their distribution is well described by Donnan equilibrium. In other words, the swelling of the gel is adjusted by varying the number of fixed charges in the gel. Surfactant–hydrogel complexing in one system of this type occurs even in the absence of an electric field, and when the gel is immersed in the surfactant solution, slow but homogeneous shrinkage of the gel is observed. The shrinkage

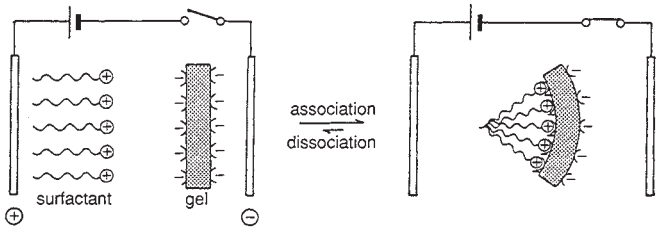

FIG. 2 Schematic illustration of bending mechanism by anisotropic association of surfactant molecules under electric field.

is attributed to the neutralization of negative charges of sulphonates in the gel by forming complexes with surfactant cations decreasing the osmotic pressure difference between the inside of the gel and the surrounding solution. Here, hydrophobic interactions between neighbouring long alkyl chains stabilize the complex and give effective contraction of the gel. We have found that an increase in alkyl chain length sharply increases the association constants of the complex.

The electric field drives and controls the direction of this equilibrium to give anisotropic complex formation. When the d.c. voltage is turned on, the positively charged surfactant molecules move by electrophoresis towards the cathode and form a complex with the negatively charged gel, preferentially on the side of the PAMPS strip facing the anode. This causes anisotropic contraction, bending the gel towards the anode (Fig. 2). When the polarity of the electric field is changed, the surfactant molecules adsorbed on the gel are released and electrophoretically travel towards the anode. Instead, new surfactant molecules form the complex preferentially on the opposite side and straighten the gel. The polymer gel can be made to bend and stretch repeatedly. It thus inches forward along the ratchet bar by means of the hooks from which it is suspended (see Fig. 1).

A moving device of this kind could serve as a new type of 'soft-actuator' or 'molecular machine'. Unlike in motors and hydrodynamic pumps, the motility of this system is produced by the chemical free energy of adsorption of surfactant molecules at the polymer network, with the electrical energy being used to drive the direction and control the state of the equilibrium. Because of the crosslinking bridges in the gel changes in molecular conformation can accumulate and lead to macroscopic shape changes. The gel-actuator also differs from piezoelectric and shape-memory materials where the shape change is caused by a phase transition. The chemomechanical gel has a gentle and flexible action resembling that of muscle rather than motion of metallic mechanical systems. □

Received 29 July; accepted 7 November 1991.

1. Katchalsky, A., Hargitay, B. & Kuhn, W. *Nature* **165**, 514-516 (1950).
2. Katchalsky, A., Oplatka, A. & Steinberg, I. Z. *Nature* **210**, 568-571 (1966).
3. Sussman, M. V. *Nature* **256**, 195-198 (1975).
4. Osada, Y. & Kishi, R. *J. chem. Soc. Faraday Trans.* **85**, 655-662 (1989).
5. Osada, Y., Yamauchi, A. & Umezawa, K. *Bull chem. Soc. Jpn* **62**, 3232-3238 (1989).
6. Flory, P.S. *Principles of Polymer Chemistry* (Cornell University Press, ithaca, New York, 1953).

ACKNOWLEDGEMENTS. We thank T. Yamamoto and Y. Kondo for providing carbon electrodes. This work was supported in part by the Science and Technology Agency, Japan.

Will greenhouse warming lead to Northern Hemisphere ice-sheet growth?

Gifford H. Miller* & Anne de Vernal†

* Center for Geochronological Research, INSTAAR, University of Colorado, Boulder, Colorado 80309-0450, USA
† GEOTOP, Université du Québec à Montréal, CP 8888, Succursale "A", Montréal, Québec, Canada, H3C 3P8

ALTHOUGH model simulations predict a higher mean global temperature by the middle of the next century in response to increased atmospheric concentrations of greenhouse gases[1], the response of the cryosphere to specific changes in latitudinal and seasonal temperature distribution is poorly constrained by modelling[2,3] or through instrumental measurements of recent variations in snow cover[4] and ice thickness[5,6]. Here we examine the recent geological record (130 kyr to present) to obtain an independent assessment of ice-sheet response to climate change. The age and distribution of glacial sediments, coupled with marine and terrestrial proxy records of climate, support arguments that initial ice-sheet growth at the beginning of the last glacial cycle occurred at high northern latitudes (65–80° N) under climate conditions rather similar to present. In particular, the conditions most favourable for glacier inception are warm high-latitude oceans, low terrestrial summer temperature and elevated winter temperature. We find that the geological data support the idea that greenhouse warming, which is expected to be most pronounced in the Arctic and in the winter months, coupled with decreasing summer insolation[7] may lead to more snow deposition than melting at high northern latitudes[8] and thus to ice-sheet growth.

Permanent ice bodies influence the heat budget of the atmosphere primarily through albedo feedback and reduction of ocean–atmosphere heat transfer[9]. The volume of land ice also controls sea level, and large continental ice sheets influence the general circulation of the atmosphere. Changes in the area and, to a lesser degree, thickness of land ice can occur rapidly. At the beginning of the last glacial cycle, ice accumulation rates were $\sim 3 \times 10^3$ km^2 yr^{-1}, accompanied by a corresponding fall in sea level of ~ 7 mm yr^{-1} (Fig. 1).

With the recognition of an anthropogenic increase in atmospher CO_2, attempt have been made to predict the climate response to these increases and possible changes in the volume of ice on the continents. The question of whether the increased melting of snow due to global warming will be offset by increased snowfall has been raised several times since the late 1970s[8] and discussed in terms of both model results[10] and direct observations[5,6], neither of which has provided a definitive answer[5,11,12]. Here we address this question from the perspective of the geological record, (1) by identifying the conditions and locus of initial ice-sheet growth in the Northern Hemisphere at the end of the last interglaciation ~120 kyr ago, and (2) from the behaviour of glaciers and ice caps during the present interglaciation (the past 10 kyr).

Terrestrial and marine records that cover the inception phase of the last interglacial (~120 to 115 kyr BP) strongly suggest that the initial build up of continental ice occurred while terrestrial climate and sea surface temperatures were close to their interglacial optima. The growth and decay of Quaternary ice sheets can be monitored on a global scale by the $\delta^{18}O$ stratigraphy in calcareous foraminifera from deep-sea sediments[13] (Fig. 1). Parallel palaeoclimatic reconstructions have been established from terrestrial and marine palaeoecological indicators that are primarily dependent on temperature. Some sites contain indications of both ice-volume variations and regional palaeoclimates. Marine microfaunal and microfloral assemblages in deep-sea cores from the North Atlantic and adjacent subpolar seas reveal the persistence of optimal sea surface temperatures after the initial increase in $\delta^{18}O$ that indicates ice accumulation on the continents at the isotope substage 5e/5d boundary[14–16]. Sites that record the evolution of terrestrial climate and sea level change through the last interglacial are reported from near-shore and terrestrial environments in the United Kingdom[17], the Netherlands[18], Germany[19] and western Norway[20], and in a marine core 100 km off the Iberian coast[21]. They show that the marine regression (indicating ice-sheet growth) began while the terrestrial climate remained close to its interglacial optimum. At the onset of the regression (rise in $\delta^{18}O$), air and sea surface temperatures around the North Atlantic and adjacent subpolar seas were nearly as warm as at present during summer and warmer than present during winter, as shown by quantitative temperature estimates based on marine microfaunal assemblages[15], terrestrial palaeovegetation records[22], and isotope composition of the Devon Island and Greenland ice cores[23,24].

The location of ice accumulation centres early in the last glaciation can be derived from the record of continental glaciation. Interstratified glacial and near-shore marine sediment along eastern Baffin Island, Canada and northern Greenland indicate that the maximum advance of the last glacial cycle occurred early, during isotope stage 5, while surface water temperatures in Baffin Bay and Labrador Sea were similar to present[25]. A similar pattern of maximum advance early in the last glaciation is recognized in Svalbard[26] and northern Alaska[27]. Early ice sheet growth over high latitude (65° to 80° N) regions of the Northern Hemisphere is supported by the pattern of ice-rafted detritus (IRD) and reworked microfossils in deep-sea sediments. A relatively high rate of IRD accumulation is recorded during isotope stage 5 in the northwestern North Atlantic[28], and reworked pre-Quaternary palynomorphs derived from glacial erosion of the Canadian High Arctic occur with maximum abundance in isotope stage 5 sediments from Baffin Bay and the Labrador Sea[16]. In addition, the isotope composition, pollen content and physical characteristics of basal ice in the Canadian Arctic ice cores suggest that the late Pleistocene ice growth started when temperatures were higher than at present, probably during the last interglacial optimum[23,29].

The possibility of high-latitude ice-sheet growth during global interglacials is illustrated by well dated records of glacial activity during the Holocene. Nearly the entire northeastern margin of the Laurentide Ice Sheet readvanced or attained its Late Wisconsin maximum during the Cockburn episode 8–9 kyr BP[30], when much of the rest of the world was close to the Holocene thermal maximum[31] and mid-latitude glaciers had already disappeared. Indeed, some local glaciers in Arctic Canada attained their maximum extension of the past 50 kyr during the little Ice Age (~1600–1900 AD)[32]. Presumably the climate of the last glacial maximum in the High Arctic was cold and very dry, inhibiting local glacier growth, whereas the warmer but wetter Holocene climate led to ice-sheet growth. Precipitation control o. glacier mass balance is well illustrated by cores through Severnaya Zemlya (Soviet Union; mean annual temperature −16 °C) ice caps which reveal maximum accumulation rates between 7 and 3 kyr BP[33], that is, during the interval of maximum northward advection of warm oceanic surface waters and moist air masses[31]. In subarctic climate zones at the same latitude (for example, Svalbard; mean annual temperature −5 °C), ice cover was markedly reduced during this interval[34]. Recent lowering